Structural and functional analyses of catalytic domain of GH10 xylanase from Thermoanaerobacterium saccharolyticum JW/SL-YS485

ARTICLE *in* PROTEINS STRUCTURE FUNCTION AND BIOINFORMATICS · JULY 2013

Impact Factor: 2.63 · DOI: 10.1002/prot.24286 · Source: PubMed

PROTEINS
STRUCTURE ■ FUNCTION ■ BIOINFORMATICS

Structural and functional analyses of catalytic domain of GH10 xylanase from *Thermoanaerobacterium saccharolyticum* JW/SL-YS485

Xu Han,[1] Jian Gao,[1] Na Shang,[1] Chun-Hsiang Huang,[1] Tzu-Ping Ko,[2] Chun-Chi Chen,[3] Hsiu-Chien Chan,[1] Ya-Shan Cheng,[4] Zhen Zhu,[1] Juergen Wiegel,[5] Wenhua Luo,[6]* Rey-Ting Guo,[1]* and Yanhe Ma[1]*

[1]Industrial Enzymes National Engineering Laboratory, Tianjin Institute of Industrial Biotechnology, Chinese Academy of Sciences, Tianjin 300308, China

[2]Institute of Biological Chemistry, Academia Sinica, Taipei 11529, Taiwan

[3]CAS Key Laboratory of Pathogenic Microbiology and Immunology, Institute of Microbiology, Chinese Academy of Sciences, Beijing 100101, China

[4]AsiaPac Biotechnology Co., Ltd., Dongguan 523808, China

[5]Department of Microbiology, University of Georgia, Athens, Georgia 30602-2605

[6]College of Food Science, South China Agricultural University, Guangzhou 510642, China

ABSTRACT

Xylanases are capable of decomposing xylans, the major components in plant cell wall, and releasing the constituent sugars for further applications. Because xylanase is widely used in various manufacturing processes, high specific activity, and thermostability are desirable. Here, the wild-type and mutant (E146A and E251A) catalytic domain of xylanase from *Thermoanaerobacterium saccharolyticum* JW/SL-YS485 (TsXylA) were expressed in *Escherichia coli* and purified subsequently. The recombinant protein showed optimal temperature and pH of 75°C and 6.5, respectively, and it remained fully active even after heat treatment at 75°C for 1 h. Furthermore, the crystal structures of apo-form wild-type TsXylA and the xylobiose-, xylotriose-, and xylotetraose-bound E146A and E251A mutants were solved by X-ray diffraction to high resolution (1.32–1.66 Å). The protein forms a classic $(\beta/\alpha)_8$ folding of typical GH10 xylanases. The ligands in substrate-binding groove as well as the interactions between sugars and active-site residues were clearly elucidated by analyzing the complex structures. According to the structural analyses, TsXylA utilizes a double displacement catalytic machinery to carry out the enzymatic reactions. In conclusion, TsXylA is effective under industrially favored conditions, and our findings provide fundamental knowledge which may contribute to further enhancement of the enzyme performance through molecular engineering.

Proteins 2013; 00:000–000

Key words: glycoside hydrolase; xylanase; crystal structure; thermophilic.

INTRODUCTION

Xylans are abundant hemicellulolytic components of plant cell wall, which can be degraded into the corresponding oligomeric and monomeric sugars, providing a major source of renewable energy. The main chain of xylan is composed of 1,4-D-xylose subunits, which is usually decorated with various side chain residues of 1,2-α-D-glucuronic acid, or its 4-*O*-methyl ethers, 1,3-α-L-arabinose, and/or *O*-acetyl groups in 2 and/or 3 position. Because of structural complexity, several xylanolytic enzymes are required to release the substituents and sugars from the various xylans, including

Grant sponsor: National Basic Research Program of China; Grand number: 2011CBA00800; Grant sponsor: National High Technology Research and Development Program of China; Grand number: 2012AA022200; Grant sponsor: Chinese Academy of Sciences; Grand number: 2011B09030042; Grant sponsor: Industrial Enzymes National Engineering Laboratory, Tianjin Institute of Industrial Biotechnology, Chinese Academy of Sciences, Tianjin 300308, China.
Xu Han, Jian Gao, and Na Shang contributed equally to this work.
*Yanhe Ma, 32 XiQiDao, Tianjin Airport Economic Park, Tianjin 300308, China. E-mail: ma_yh@tib.cas.cn or Rey-Ting Guo, 32 XiQiDao, Tianjin Airport Economic Park, Tianjin 300308, China. E-mail: guo_rt@tib.cas.cn or Wenhua Luo, No. 3 Gongye North Road, Songshan Lake Scientific Industrial Park, Dongguan, Guangdong Province, China. E-mail: wenhualuo@126.com
Received 3 January 2013; Revised 1 March 2013; Accepted 5 March 2013
Published online 18 March 2013 in Wiley Online Library (wileyonlinelibrary.com). DOI: 10.1002/prot.24286

endo-1,4-β-xylanases (EC 3.2.1.8), acetyl xylan esterases (EC 3.1.1.72), feruloyl esterases (EC 3.1.1.73), α-L-arabinofuranosidases (EC 3.2.1.55), α-glucuronidases (EC 3.2.1.139), and β-D-xylosidase (EC 3.2.1.37). Among these enzymes, endo-1,4-β-xylanases are believed to be the most valuable in industrial applications.

Endo-1,4-β-xylanases (EC 3.2.1.8) hydrolyze the internal β-1,4-xylosidic bonds within the main chain of xylan to release the sugars. According to their protein sequence homology, most xylanases are classified into the glycoside hydrolase (GH) family 10 and 11, while others belong to the GH5, GH7, GH8, and GH43 families (http://www.cazy.org/Glycoside-Hydrolases.html). Xylanses have been widely used in biotechnological applications including paper manufacturing,[1] food processing,[2] feedstock additive,[3] and biofuel production.[4] For these industrial processes, thermostability is a desirable property for xylanase, yet most commercial utilized enzymes are mesophilic proteins. Direct evolution involving error-prone PCR is a powerful tool to obtain a library for subsequent screening for new proteins with potential enhanced thermostability, but the procedures are laborious. An alternative way to improve enzyme performance is by rational engineering which is operated through introducing unique structural features to proper positions. However, this technique requires specific protein structural information. In our previous studies, this method has proved feasible in increasing enzyme activities.[5–7] On the other hand, searches for novel thermophilic enzymes from extremophiles as a starting point have been an important approach to obtain industrial useful enzymes.

Several xylanases from various thermophilic microorganisms have been characterized, and some of their crystal structures with or without substrates have been solved.[8] *Thermoanaerobacterium saccharolyticum* JW/SL-YS485 is a thermophilic anaerobic bacterium that grows in a broad range of pH (3.85–6.35) and temperature (30–66°C) and can use xylan as the sole carbon and energy source.[9] Several hemicellulolytic enzymes of this bacterial strain have been identified and characterized including two acetyl xylan esterases,[10] an α-*O*-methylglucuronidase,[11] a large cell-associated endoxylanase,[12,13] and three xylosidases.[14–17] The *T. saccharolyticum* JW/SL-YS485 endoxylanase (TsXynA) belongs to GH10 family and has the highest molecular weight (more than 150 kDa) among all cell-associated xylanases.[12,13] It is composed of an N-terminal modular domain (two carbohydrate binding domains; CBD), a catalytic domain, and three S-layer repeats on the C-terminus. It shows optimum activity at 80°C and pH 6.3, and has a half-life of 1 h at 77°C.[13] Despite the great potential of TsXynA in industrial applications, its unusually large size and cell-associated properties could cause inefficient production and high manufacturing cost. In our previous study, enzyme performances could be significantly improved by truncating regulatory domains, and the truncated enzyme can be further modified for better industrial applications based on the structural information.[5,18] In this study, the catalytic domain of TsXynA was cloned and expressed in *E. coli*, dubbed TsXylA here. The enzyme activity and thermostability were then investigated. In particular, the crystal structures of the apo-form and ligand-bound TsXylA were solved at high resolution of 1.32–1.66 Å to reveal the overall protein folding and the residues involved in substrate binding. A catalytic mechanism is also proposed by analyzing the complex structures. This study increases our knowledge about the molecular basis of thermophilic xylanases, and the truncated thermophilic xylanase may benefit future biotechnological applications.

MATERIALS AND METHODS

Materials

The *PfuTurbo* DNA polymerase was obtained from Life Technologies. The plasmid mini-prep kit and DNA gel extraction kit were purchased from Qiagen. The Ni-NTA resin was purchased from GE Healthcare. The protein expression kit (the pET46 Ek/LIC vector) and the *E. coli* DH5α and *E. coli* BL21 (DE3) competent cells were purchased from Novagen. The QuickChange Site-Directed Mutagenesis Kit was obtained from Agilent Technologies. Beechwood xylan was purchased from Sigma.

Cloning of the xylanase gene

The cloning of a conserved catalytic region from the whole *xylA* gene of *T. saccharolyticum* JW/SL-YS485 was carried out following the instructions of pET46 EK/LIC vector kit manual. The gene fragment coding TsXylA was amplified by polymerase chain reaction (PCR) using a forward primer of 5′-GACGACGACAAGATGACAATACAAAATGATATTCCGGATTTA-3′ and a reverse primer of 5′-GAGGAGAAGCCCGGTTATGCAGATTGAATGTCAGGTATGGCTTT-3′. The E146A and E251A mutants were created by using QuickChange Site-Directed Mutagenesis Kit with TsXylA-pET46 EK/LIC gene as the template. The mutagenic oligonucleotides were 5′-GGATGGGATGTTGTAAAT**GCT**GTTCTTGATGATAATGGC-3′ for E146A, and 5′-GTGGAAATACAGGTAACT**GCT**TTAGATATGAACATGAATGGT-3′ for E251A. The constructs were transformed to *E. coli* BL21 (DE3) for protein expression.

Overexpression and purification of enzyme

The recombinant protein expression was induced with 1 m*M* isopropyl β-thiogalactopyranoside (IPTG) at 18°C for 24 h. Cell paste was harvested by centrifugation at 7000*g* and resuspended in a lysis buffer containing 25

Table I
Data Collection and Refinement Statistics for TsXylA Crystals

	w.t. apo	E146A- xylobiose	E146A- xylotriose	E251A- xylobiose	E251A- xylotriose	E251A- xylotetraose
PDB code	3W24	3W25	3W26	3W27	3W28	3W29
Data co1lection						
Space group	$P2_12_12$	$P2_12_12$	$P2_12_12$	$P2_12_12$	$P2_12_12$	$P2_12_12$
Unit-cell						
a [Å]	76.9	77.1	77.1	77.4	77.4	77.3
b [Å]	118.8	118.6	118.4	119.2	119.2	119.4
c [Å]	45.3	45.4	45.4	45.4	45.4	45.4
Resolution [Å][a]	25–1.35 (1.40–1.35)	25–1.32 (1.37–1.32)	25–1.60 (1.66–1.60)	25–1.41 (1.46–1.41)	25–1.39 (1.44–1.39)	25–1.39 (1.44–1.39)
No. of unique reflections	90,031 (9102)	98,337 (9720)	55,315 (5410)	81,686 (8047)	84274 (8214)	83,501 (8097)
Redundancy	3.6 (3.6)	7.0 (6.8)	6.5 (6.0)	7.0 (7.2)	7.2 (7.3)	6.7 (6.8)
completeness [%]	97.6 (100.0)	99.8 (99.9)	99.4 (98.6)	99.9 (99.6)	98.8 (97.5)	97.7 (96.0)
Average $I/\sigma(I)$	21.8 (3.8)	20.6 (3.3)	19.7 (4.6)	24.0 (3.3)	25.4 (3.8)	20.0 (4.2)
R_{merge} [%]	6.2 (48.1)	10.3 (46.6)	10.9 (40.4)	8.8 (52.0)	8.4 (48.7)	10.2 (45.1)
Refinement						
R_{work}	0.175 (0.242)	0.163 (0.220)	0.163 (0.214)	0.179 (0.254)	0.171 (0.232)	0.177 (0.239)
R_{free}	0.198 (0.247)	0.184 (0.239)	0.186 (0.231)	0.197 (0.254)	0.191 (0.244)	0.210 (0.265)
r.m.s.d. bonds [Å]	0.023	0.026	0.006	0.011	0.011	0.021
r.m.s.d. angles [°]	2.3	2.2	1.4	1.6	1.6	2.0
dihedral angles						
most favored [%]	90.4	91.4	90.0	92.1	91.8	91.4
allowed [%]	9.3	8.6	10.0	7.9	8.2	8.6
disallowed [%]	0.3	0	0	0	0	0
No. of non-H atoms / average B [Å^2]						
Protein	2598/12.7	2594/11.8	2594/14.5	2594/15.2	2594/13.8	2594/14.0
Water	607/29.8	691/29.1	827/38.1	674/32.9	689/32.2	752/34.9
Ligand		19/7.2	28/13.1	19/10.2	28/12.6	37/18.1

[a]Values in the parentheses are for the highest resolution shells.

m*M* Tris, pH 7.5, 150 m*M* NaCl and 20 m*M* imidazole. Cell lysates were prepared with a JNBIO® pressure cell (JN-3000 PLUS), and then centrifuged at 17,000*g* to remove cell debris. The cell-free extract was loaded onto a lysis buffer-equilibrated Ni-NTA column. The column was washed with a buffer containing 25 m*M* Tris, pH 7.5, 150 m*M* NaCl and 20 m*M* imidazole. The His-tagged enzyme was eluted using a 20–250 m*M* imidazole gradient, the pooled fractions dialyzed twice against 5 L of 25 m*M* Tris, pH 7.5, and then loaded into a 20 mL DEAE Sepharose Fast Flow column (GE Healthcare Life Sciences). The buffer and gradient were 25 m*M* Tris, pH 7.5, and 0–500 m*M* NaCl. The purity of recombinant proteins (>95%) was checked by SDS-PAGE analysis.

Enzyme activity assay

Xylanase activity was estimated by determining the amount of reducing sugars released from beechwood xylan (Sigma) by the 3,5-dinitrosalicylic acid (DNS) protocol using xylose as a standard.[19] The xylanase activity was calculated as international units (U), the amount of enzyme which released 1 µmol product per minute. The reaction assay mixture (2 mL) consisted of 1.0% beechwood xylan and suitably diluted enzyme solution (0.2 mL) in a 50 mM sodium acetate acetic acid buffer solution, pH 5.3. The optimal pH of TsXylA was determined as pH 6.5 when the reaction was conducted at 75°C for 10 min. Afterward, the optimal temperature and thermostability for TsXylA was determined at pH 6.5.

Crystallization and data collection

Initial crystallization screening was performed using Hampton Research Crystal Screens Kit (Laguna Niguel, CA) with the sitting-drop method at room temperature. In general, 2 µL TsXylA protein solution (10 mg mL^{-1} TsXylA enzyme, 25 m*M* Tris, pH 7.5 and 150 m*M* NaCl)

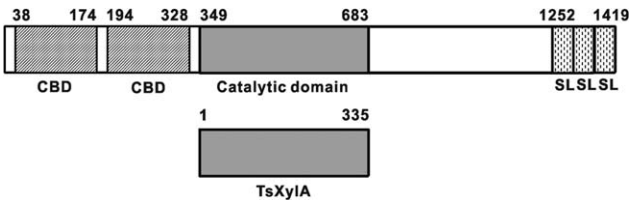

Scheme 1
Schematic representation of full length and truncated amino acid residues 349–683 xylanase (CBD: Carbohydrate Binding Domain; SL: S-Layer Homology Domain).

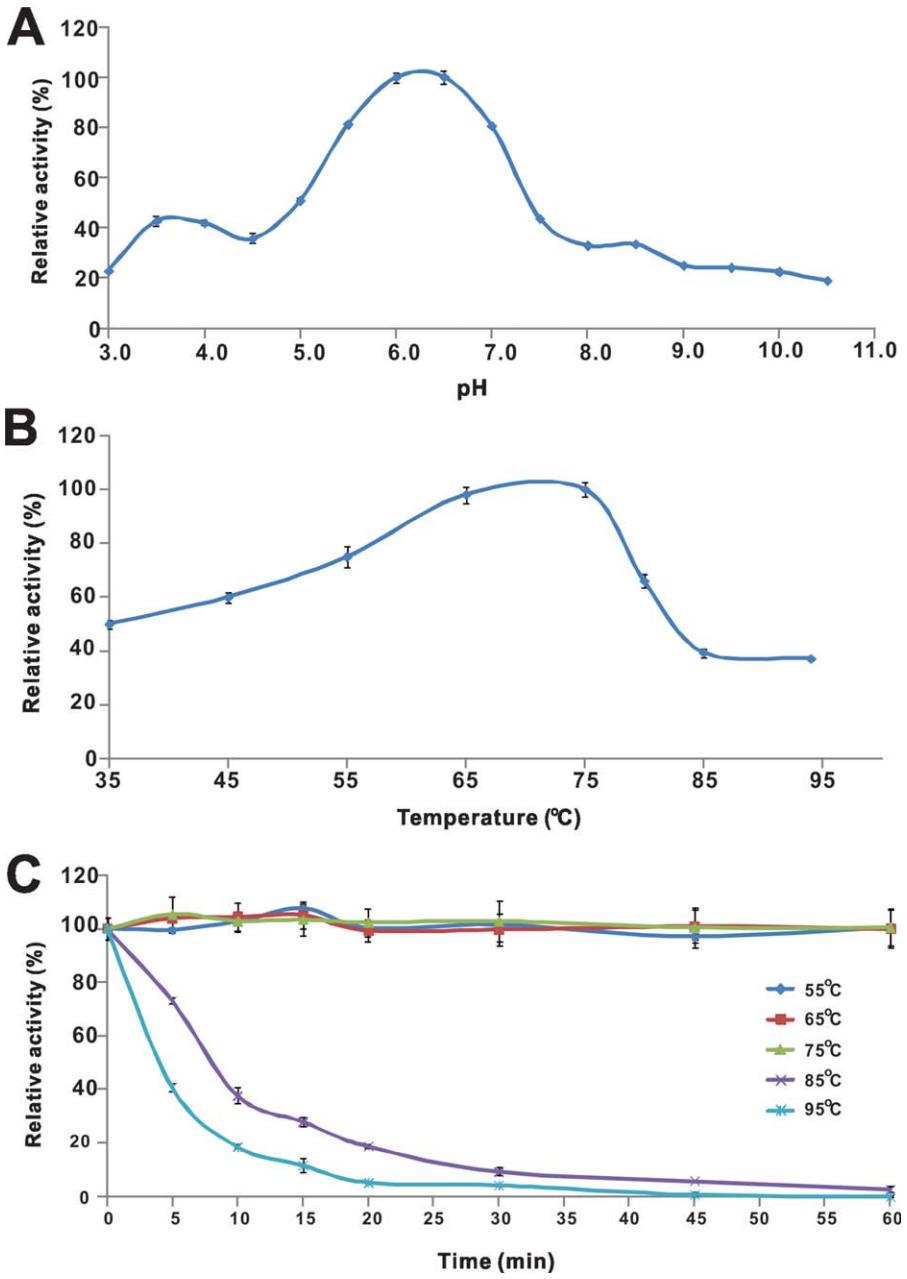

Figure 1

The pH/temperature effects and thermostability of TsXylA. (**A**) The pH dependence of the TsXylA activity was determined using di-sodium hydrogen phosphate-citrate buffer (pH 3.0–8.0), Tris-HCl buffer (pH 8.5–9.0) and sodium carbonate-sodium bicarbonate buffer (pH 9.5–10.5) at 75°C. (**B**) The enzyme activity of recombinant TsXylA was measured at 35, 45, 55, 65, 75, 85, and 95°C (pH 5.3). (**C**) To estimate the thermostability, the TsXylA was pre-incubated at different temperatures for indicated time periods before enzyme activity was determined (pH 6.0). All experiments were carried out in triplicates, and the activity was calculated as percentage of maximal values and presented as average ± SD.

was mixed with 2 μL of reservoir solution. Single crystal was obtained in 0.1*M* Tris, pH 8.0, 25% PEG 6000 and 0.8*M* LiCl. Prior to data collection, the crystals were mounted in a cryoloop and flash-frozen in liquid nitrogen with 0.15*M* Tris, pH 8.0, 30% PEG 6000 and 1.5*M* LiCl as a cryoprotectant.

Attempts to obtain the structure of wild-type protein in complex with ligands failed. To understand the ligand binding mode, two mutations of the catalytic residues (E146A and E251A) were introduced for obtaining ligand complex structures. The E146A and E251A proteins exhibited no enzyme activity (data not shown). The

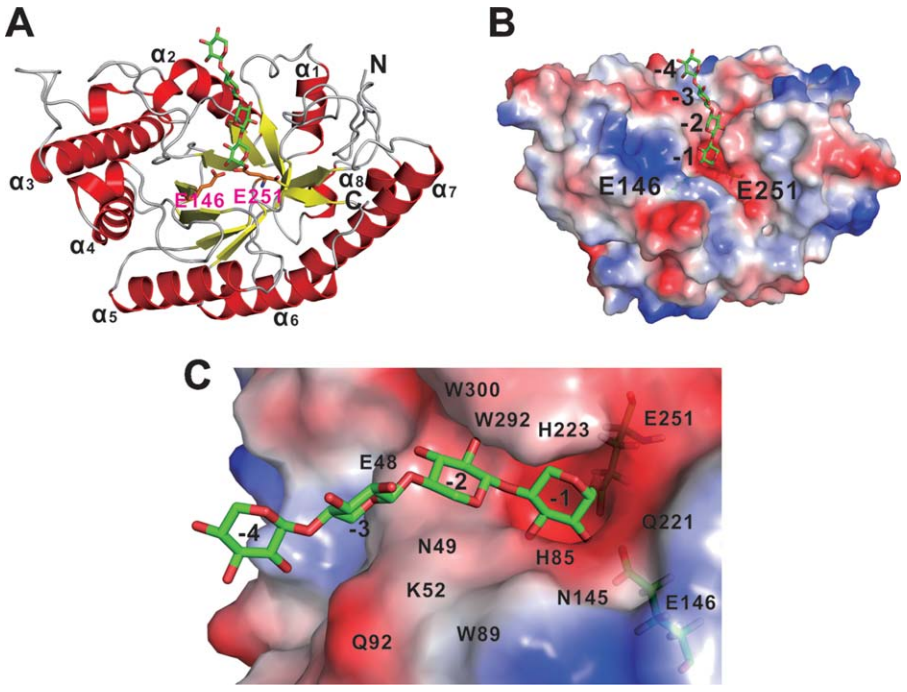

Figure 2

Overall crystal structures of substrate-bound TsXylA. (**A**) The polypeptide chain of the enzyme. All α-helices and β-sheets are colored in yellow and red, and two catalytic glutamates (E146 and E251) are shown as sticks. Xylotetraose (from E251A-xylotetraose complex structure) is modeled into the wild type apo-form structure and shown as sticks also. (**B**) Surface representation and xylotetraose-binding mode of TsXylA. The protein is shown using the molecular electrostatic surface, with red for negative charge and blue for positive charge. (**C**) Molecular surface of the xylotetraose-binding groove of TsXylA. Color presentation is as in panel (B). Residues which involved in the substrate-binding tunnel are labeled.

crystallization conditions of E146A and E251A mutants are similar to that of the wild-type xylanase. The E146A and E251A crystals were obtained in 0.1*M* Tris, pH 8.0, 23–26% PEG 6000 and 0.7–0.8*M* LiCl. The crystals of E146A and E251A in complex with xylobiose, xylotriose, and xylotetraose were obtained by soaking the crystals with the cryoprotectant solution (0.15*M* Tris, pH 8.0, 30% PEG 6000 and 1.5*M* LiCl) that contained 10 m*M* ligands.

The diffraction data from these crystals were collected at beam line BL13B1 and BL13C1 of the National Synchrotron Radiation Research Center (NSRRC, Hsinchu, Taiwan), and processed using the programs of HKL2000.[20] Prior to structural refinements, 5% randomly selected reflections were set aside for calculating R_{free} as a monitor.[21]

Structure determination and refinement

The native TsXylA structure was solved by molecular replacement (MR) method using the CNS program.[22] The intracellular xylanase from *Geobacillus stearothermophilus* structure (PDB code 2Q8X) was used as a search model (with 46% identity). The complex structures were solved by MR using the refined TsXylA as a search model.

All of the orthorhombic crystals belong to $P2_12_12$ space group and contain one TsXylA molecule in an asymmetric unit. Subsequent incorporation of ligands (xylobiose, xylotriose, and xylotetraose) and water molecules were performed according to 1.0 σ map level. Some data collection statistics are listed in Table I. All the structural refinements were done with Coot[23] and CNS program.[22] All of the structural diagrams were drawn using PyMol (http://pymol.sourceforge.net/).

RESULTS AND DISCUSSIONS

Enzymatic activity

The catalytic domain of TsXynA from amino acid residues 349 to 683 (TsXylA; Scheme 1) was cloned, expressed and purified from *E. coli*, and the xylanase activity was examined. The optimal pH range for TsXylA is between 6.0 and 6.5 at 75°C, while more than 80% activity was detected at pH ranging from 5.5 to 7.0 [Fig. 1(A,B)]. To test TsXylA thermostability, the protein was incubated at different temperatures for various time periods before activity measurements. As shown in Figure 1(C), we found that the TsXylA remained fully active even after being heated at 75°C for as long as 1 h, but

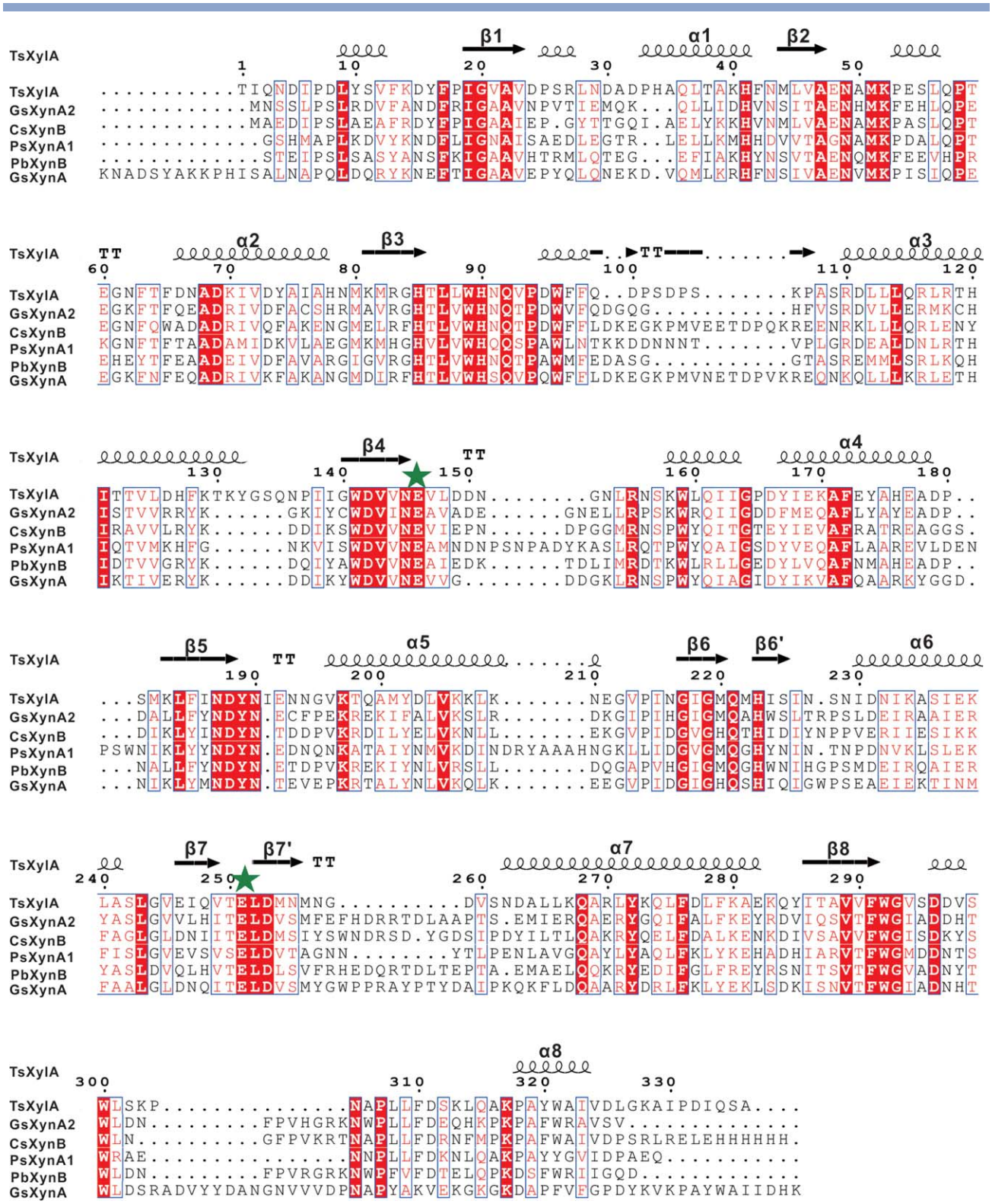

Figure 3

Amino acid alignment of TsXylA and other GH10 xylanases. The alignment includes xylanases from *T. thermosulfurigenes*, (TsXylA), *G. stearothermophilus* (GsXynA2, PDB code 2Q8X), *C. sterocorarium* (CsXynB, PDB code 2DEP), *Paenibacillus* sp. (PsXynA1, PDB code 3RDK), *P. bacinonensis* (PbXynB, PDB code 3EMC), *G. stearothermophilus* (GsXyn, PDB code 1R87). Strictly conserved residues are highlighted by red background and conservatively substituted residues are boxed. The secondary structural elements (helices-α, strands-β, turns-T) of TsXylA are shown above the aligned sequences. The conserved catalytic residues E146 and E251 are indicated by green asterisks. The figure was produced using ESPript.[25,26]

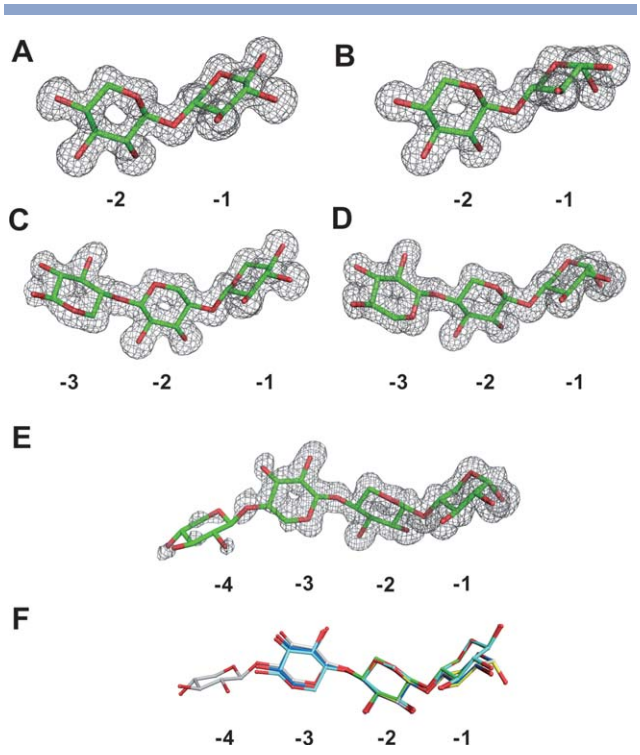

Figure 4

The electron density map and superimposition of all substrates observed in this study. The *Fo-Fc* omit maps of (**A**) xylobiose from the E146A-xylobiose structure, (**B**) xylobiose from the E251A-xylobiose structure, (**C**) xylotriose from the E146A-xylotriose structure, (**D**) xylotriose from the E251A-xylotriose structure, and (**E**) xylotetraose from the E251A-xylotetraose structure are contoured at 3 σ level and colored in gray, respectively. (**F**) All bound ligands in the E146A or E251A mutant crystals, including xylobiose, xylotriose, and xylotetraose, are superimposed. E146A-xylobiose, E251A-xylobiose, E146A-xylotriose, E251A-xylotriose, and E251A-xylotetraose are colored in green, yellow, aquamarine, blue, and grey, respectively. Subsites are numbered below the substrates in all panels.

the stability sharply declined beyond 85°C. According to these results, the enzymatic activity is preserved for the truncated TsXylA protein as it shares similar temperature and pH profiles with full-length TsXynA.[12,13] Notably, there was a minor peak of specific activity observed between pH 3.0 to 4.5 where about 40% of the maximal value was detected [Fig. 1(A)]. This is not observed in previous studies with full-length protein and suggests TsXylA may be able to operate in acidic environment. Whether domain truncations contribute to the phenomena needs further examination to clarify. According to these results, the recombinant TsXylA shows enzymatic activity and possesses excellent thermostability as the original full-length enzyme.

Overall structure

When the crystal structure of wild-type TsXylA was solved in the presence of all substrates used in this study, no ligands were seen. Two glutamates, E146 and E251, were identified as the catalytic residues according to sequence homology analysis[24] [Figs. 2(A) and 3)]. Subsequently the inactive mutants E146A and E251A were expressed and purified to obtain ligand-bound structures. Altogether, we solved the crystal structures of a wild-type TsXylA (w.t. apo) and five ligand-bound mutants (E146A-xylobiose, E146A-xylotriose, E251A-xylobiose, E251A-xylotriose, and E251A-xylotetraose). These structures have the same space group ($P2_12_12$) and similar cell dimensions, and all show a typical $(\beta/\alpha)_8$ TIM-barrel fold [Table I, and Fig. 2(A)]. The numbering of α-helices (α_n) and β-strands (β_n) is assigned according to the classical arrangement of eight α-helices (α_1–α_8) in the external part and eight β-strands (β_1–β_8) in the internal core of the protein [Figs. 2(A) and 3]. The ligand-bound structures superimpose very well with the apo-form structure by root-mean-square deviations (RMSD) ranging from 0.099 to 0.111 for all Cα atoms, indicating the protein conformation was not significantly altered upon substrate binding.

Similar to most other GH10 xylanases, TsXylA forms an open cleft on the protein surface on the carboxyl-terminal side of the internal barrel [Fig. 2(B)]. This groove is exposed to the solvent, and aromatic and hydrophilic residues line the inner wall of the tunnel, which may participate in the interaction with the substrate sugar moieties [Fig. 2(C)]. E146 and E251, located on the substrate-binding cleft surface opposing each other, are predicted as conserved catalytic residues [Fig. 2(A)]. Similar to the other GH10 xylanases, TsXylA has the two catalytic glutamates on the carboxyl-terminus of strand β_4 and the β-bulge on strand β_7 [Fig. 2(A) and 3].

Catalytic domain structure

The electron densities of the ligands (xylobiose, xylotriose, and xylotetraose) are clear in E146A and E251A complex crystals [Fig. 4(A–E)]. The xylose residues are clearly seen at 3.0 σ level in the high resolution E146A-xylobiose (1.32 Å) and E251A-xylobiose (1.41 Å) structures, whereas the densities for sugar in the −4 subsite are much weaker in E251A-xylotetraose structure. Weaker densities observed in these subsites are supported by their binding patterns, as the −4 sugars hang loosely at the open end of the groove while the −1, −2, and −3 sugars are tightly fixed deep in the tunnel [Fig. 2(B)]. Xylobiose, xylotriose and xylotetraose are found to occupy subsites −2 to −1, −3 to −1, and −4 to −1, respectively, whereas no density in aglycon region was visible. To reveal −4 to −1 subsites, all the ligands are superimposed [Fig. 4(F)]. The sugar in subsite −1 shows no better superimposition than −2 and −3 although it exhibits electron density as strong as the −2 sugar. This result is due to the orientation of one hydroxyl group in

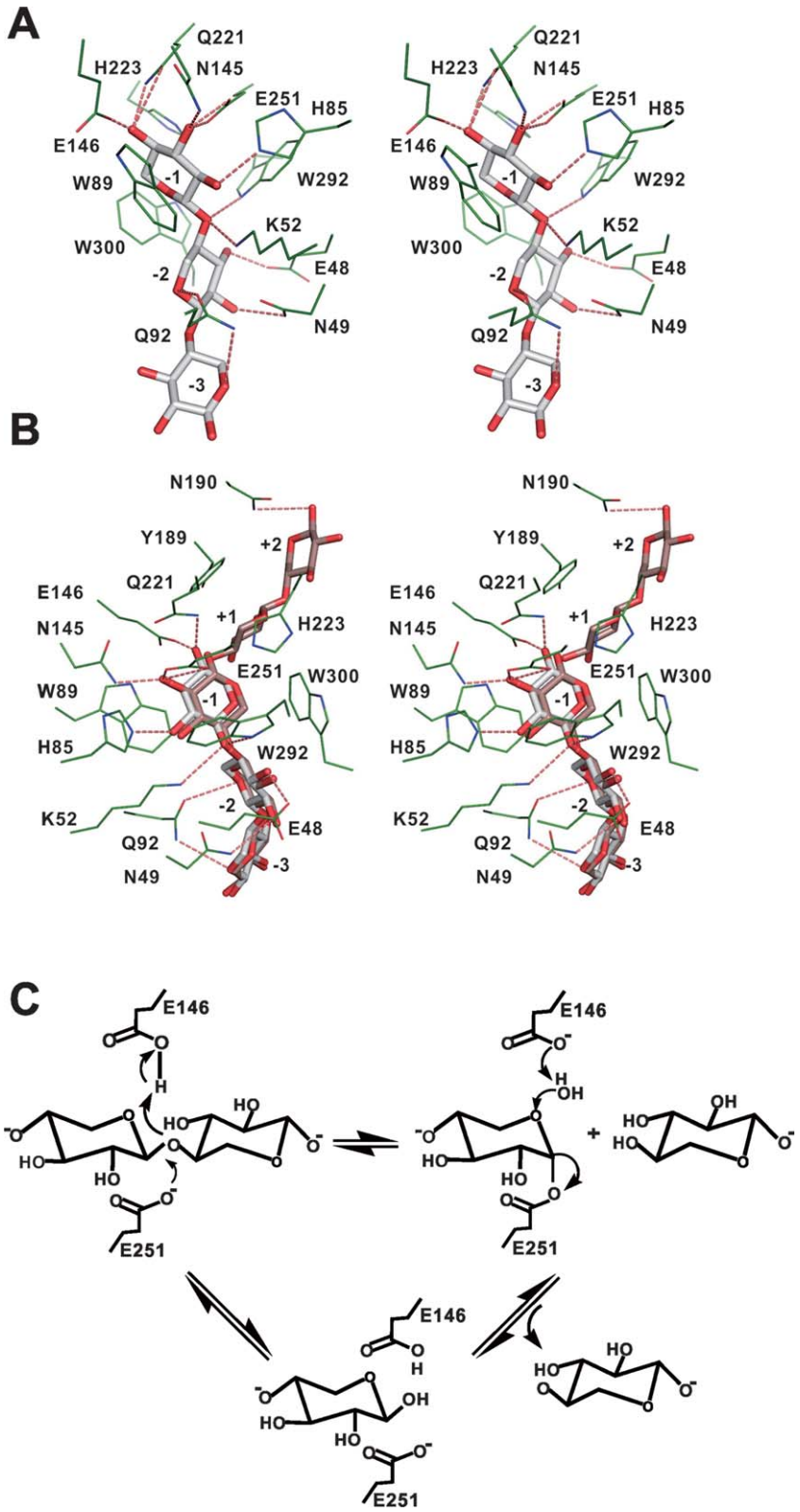

Figure 5

Detailed interaction networks in the active site and proposed catalytic mechanism. (**A**) A stereo view of detailed interaction networks of the TsXylA active site residues with xylotriose (from E146A-xylotriose structure; colored in white). Hydrogen bonds with a distance below 3.5 Å are shown as red dashed lines. (**B**) A stereo view of active site networks by superimposition of E146A-xylotriose with xylopentaose (light orange) from the GsXynA complex structure (PDB 1R87). The xylopentaose occupying subsites +2 to −3 and the interacting residues are shown. (C) Proposed catalytic mechanism for TsXylA.

the −1 sugar, which is toward the E251 position in E146A but toward the E146 position in E251A.

The detailed interactions between the active site residues of E146A with xylotriose are depicted in Figure 5(A). W89 and H223 provide stacking forces for the −1 sugar with an interplanar distance of 4.0–5.0 Å. Hydrogen bonds provided by H85, N145, Q221, and W292 also aid to form subsite −1. Stacking forces from W300 together with hydrogen bonds provided by E48, N49, and K52 form subsite −2. Weaker interaction was observed for the −3 sugar that only Q92 provides an evident hydrogen bond. A superposition of xylopentaose with E146-xylotriose reveals potential aglycon subsites of TsXylA. Here subsite +1 is formed by Y189 and subsite +2 is formed by N190 [Fig. 5(B)].

As GH10 xylanases are retaining glycoside hydrolases, TsXylA is supposed to function via the same catalytic procedures. From sequence analysis and previous studies, E251 is the nucleophile and E146 is the general acid/base[27] (Fig. 3). First, E146 functions as a general acid to protonate the glycosidic oxygen and E251 attacks the anomeric center as a nucleophile to generate the glycosyl-enzyme intermediate. In the next step, the deprotoned E146 becomes a general base to attract a proton from a water molecule which then hydrolyzes the glycosyl-enzyme intermediate to leave a net retention anomeric configuration [Fig. 5(C)].

In conclusion, we have identified and characterized a new thermophilic xylanase from a xylanolytic bacterium. The crystal structure analysis reveals its folding and substrate-binding pattern. It is believed that in the future the enzyme TsXylA could be used in some industrial applications.

REFERENCES

1. Bajpai P. Application of enzymes in the pulp and paper industry. Biotechnol Prog 1999;15:147–157.
2. Olempska-Beer ZS, Merker RI, Ditto MD, DiNovi MJ. Food-processing enzymes from recombinant microorganisms—a review. Regul Toxicol Pharmacol 2006;45:144–158.
3. Prade RA. Xylanases: from biology to biotechnology. Biotechnol Genet Eng Rev 1996;13:101–131.
4. Dodd D, Cann IK. Enzymatic deconstruction of xylan for biofuel production. Glob Change Biol Bioenergy 2009;1:2–17.
5. Huang JW, Cheng YS, Ko TP, Lin CY, Lai HL, Chen CC, Ma Y, Zheng Y, Huang CH, Zou P, Liu JR, Guo RT. Rational design to improve thermostability and specific activity of the truncated *Fibrobacter succinogenes* 1,3-1,4-beta-D-glucanase. Appl Microbiol Biotechnol 2012;94:111–121.
6. Cheng YS, Ko TP, Wu TH, Ma Y, Huang CH, Lai HL, Wang AHJ, Liu JR, Guo RT. Crystal structure and substrate-binding mode of cellulase 12A from *Thermotoga maritima*. Proteins Struct Funct Bioinform 2011;79:1193–1204.
7. Cheng YS, Ko TP, Huang JW, Wu TH, Lin CY, Luo W, Li Q, Ma Y, Huang CH, Wang AJ, Liu JR, Guo RT. Enhanced activity of *Thermotoga maritima* cellulase 12A by mutating a unique surface loop. Appl Microbiol Biotechnol 2012;95:661–669.
8. Collins T, Gerday C, Feller G. Xylanases, xylanase families and extremophilic xylanases. FEMS Microbiol Rev 2005;29:3–23.
9. Lee YE, Jain MK, Lee C, Zeikus JG. Taxonomic distinction of saccharolytic thermophilic anaerobes: description of *Thermoanaerobacterium xylanolyticum* gen. nov., sp. nov., and *Thermoanaerobacterium saccharolyticum* gen. nov., sp. nov.; Reclassification of *Thermoanaerobium brockii, Clostridium thermosulfurogenes*, and *Clostridium thermohydrosulfuricum* E100-69 as *Thermoanaerobacter brockii* comb. nov., *Thermoanaerobacterium thermosulfurigenes* comb. nov., and *Thermoanaerobacter thermohydrosulfuricus* comb. nov., Respectively; and Transfer of *Clostridium thermohydrosulfuricum* 39E to *Thermoanaerobacter ethanolicus*. Int J Syst Bacteriol 1993;43:41–51.
10. Shao W, Wiegel J. Purification and characterization of two thermostable acetyl xylan esterases from *Thermoanaerobacterium* sp. strain JW/SL-YS485. Appl Environ Microbiol 1995;61:729–733.
11. Shao W, Obi S, Puls J, Wiegel J. Purification and characterization of the (alpha)-glucuronidase from *Thermoanaerobacterium* sp. strain JW/SL-YS485, an important enzyme for the utilization of substituted xylans. Appl Environ Microbiol 1995;61:1077–1081.
12. Shao W, Deblois S, Wiegel J. A high-molecular-weight, cell-associated xylanase isolated from exponentially growing *Thermoanaerobacterium* sp. strain JW/SL-YS485. Appl Environ Microbiol 1995;61:937–940.
13. Liu SY, Gherardini FC, Matuschek M, Bahl H, Wiegel J. Cloning, sequencing, and expression of the gene encoding a large S-layer-associated endoxylanase from *Thermoanaerobacterium* sp. strain JW/SL-YS 485 in *Escherichia coli*. J Bacteriol 1996;178:1539–1547.
14. Huang CH, Sun Y, Ko TP, Chen CC, Zheng Y, Chan HC, Pang X, Wiegel J, Shao W, Guo RT. The substrate/product-binding modes of a novel GH120 beta-xylosidase (XylC) from *Thermoanaerobacterium saccharolyticum* JW/SL-YS485. Biochem J 2012;448:401–407.
15. Liu W, Sun Y, Ko TP, Wiegel J, Shao W, Lu F, Guo RT, Huang CH. Crystallization and preliminary X-ray diffraction analysis of a novel GH120 beta-xylosidase (XylC) from *Thermoanaerobacterium saccharolyticum* JW/SL-YS485. Acta Crystallogr Sect F Struct Biol Crystallization Commun 2012;68:914–916.
16. Shao W, Xue Y, Wu A, Kataeva I, Pei J, Wu H, Wiegel J. Characterization of a novel beta-xylosidase, XylC, from *Thermoanaerobacterium saccharolyticum* JW/SL-YS485. Appl Environ Microbiol 2011;77:719–726.
17. Lorenz WW, Wiegel J. Isolation, analysis, and expression of two genes from *Thermoanaerobacterium* sp. strain JW/SL YS485: a beta-xylosidase and a novel acetyl xylan esterase with cephalosporin C deacetylase activity. J Bacteriol 1997;179:5436–5441.
18. Wen TN, Chen JL, Lee SH, Yang NS, Shyur LF. A truncated fibrobacter succinogenes 1,3-1,4-beta-D-glucanase with improved enzymatic activity and thermotolerance. Biochemistry 2005;44:9197–9205.
19. Miller G. Cardiac arrest. Miss Doct 1959;37:149–151.
20. Zbyszek O, Wladek M. Processing of X-ray diffraction data collected in oscillation mode. Methods Enzymol 1997;276:307–326.
21. Brunger AT. Assessment of phase accuracy by cross validation: the free R value. Methods and applications. Acta Crystallogr D Biol Crystallogr 1993;49:24–36.
22. Brunger AT, Adams PD, Clore GM, DeLano WL, Gros P, Grosse-Kunstleve RW, Jiang JS, Kuszewski J, Nilges M, Pannu NS, Read RJ, Rice LM, Simonson T, Warren GL. Crystallography and NMR system: a new software suite for macromolecular structure determination. Acta Crystallogr D Biol Crystallogr 1998;54:905–921.

23. Emsley P, Lohkamp B, Scott WG, Cowtan K. Features and development of Coot. Acta Crystallogr D Biol Crystallogr 2010;66:486–501.
24. Solomon V, Teplitsky A, Shulami S, Zolotnitsky G, Shoham Y, Shoham G. Structure-specificity relationships of an intracellular xylanase from Geobacillus stearothermophilus. Acta Crystallogr D Biol Crystallogr 2007;63:845–859.
25. Thompson JD, Gibson TJ, Plewniak F, Jeanmougin F, Higgins DG. The CLUSTAL_X windows interface: flexible strategies for multiple sequence alignment aided by quality analysis tools. Nucleic Acids Res 1997;25:4876–4882.
26. Gouet P, Robert X, Courcelle E. ESPript/ENDscript: extracting and rendering sequence and 3D information from atomic structures of proteins. Nucleic Acids Res 2003;31:3320–3323.
27. Davies G, Henrissat B. Structures and mechanisms of glycosyl hydrolases. Structure 1995;3:853–859.